JOURNAL OF AIRCRAFT
Vol. 35, No. 2, March–April 1998

Composite Patches as Reinforcements and Crack Arrestors in Aircraft Structures

M. R. Lena,* J. C. Klug,† and C. T. Sun‡
Purdue University, West Lafayette, Indiana 47906-1282

The application of adhesively bonded composite patches as reinforcements and crack arrestors for a multisite damaged aircraft structure is investigated. Experiments are performed to test the ability of a bonded composite reinforcement to prevent cracks from coalescing. With a finite element model developed for composite patch repairs, the effect of thermal residual stresses on the stress-intensity factor and the resulting fatigue crack growth rate is demonstrated. An effective thermal stress is estimated by comparing experimental results with model predictions. Reinforcement for a multiple-site damage situation is analyzed by modeling an infinite row of closely spaced cracked rivet holes. The composite reinforcement is shown to dramatically reduce the stress-intensity factor, increase fatigue life, and protect against catastrophic failure.

I. Introduction

OWING to their high-stiffness, high-strength, and lightweight properties, advanced fiber composites have found a new application in repairing aging aircraft through patching.[1] These repairs can be quickly applied on-site to the aircraft structure, drastically reducing the large costs associated with disassembly and downtime. One important characteristic of aircraft structures is damage tolerance. To obtain a complete understanding of the damage tolerance of a repair, simple models must be employed that can capture the primary mechanisms leading to and affecting failure.

Bonded composite repair has been recognized as an efficient and economical method to extend the service life of cracked aluminum components. The current applications of composite repairs have been summarized in Refs. 1–3. Composite repair has taken numerous roles on military aircraft, such as a reinforcement in areas where stress corrosion cracking can occur, as on the lower surface of the wing pivot on a U.S. Air Force F-111, or fatigue cracking around a fuel decant hole on a Royal Australian Air Force (RAAF) Mirage III. On commercial aircraft, the use of composite repairs is in early stages.[3] The composite is installed as a decal on key areas of the aircraft to determine whether the repair can handle various effects of flight exposure, including cabin pressurizations, environmental and fluid exposure, and aerodynamic loading.

One of the key issues in aircraft failure is the presence of multiple cracks in a local area, known as multisite damage (MSD). Analysis of the repair of MSD has been proposed by Park et al.[4] by placing a patch over a cracked pin-loaded fastener hole. The finite element alternating method was used, and fastener loading and flexibility were taken into account.

In this paper, the composite is not placed directly over the crack; instead, it is used as a reinforcement in protecting against crack initiation. The composite is bonded between two cracks to try to prevent the cracks from coalescing. Specifically, symmetric (double-sided) reinforcements are tested, and a finite element model is developed to solve for the stress-intensity factor as a function of crack length. By numerically integrating the Paris law, the fatigue life is estimated and compared with experimental data.

The adhesive bonding process requires curing at an elevated temperature. There is a significant thermal mismatch between aluminum and the composite material, resulting in thermal residual stresses. A residual tension is left in the aluminum, increasing the stress-intensity factor and shortening fatigue life. The thermal residual stresses must be quantified to estimate fatigue life.

In this study, two configurations of cracked aluminum plates are considered. The first is a double-edge-cracked specimen with a composite strip placed at the center separating the two cracks. The second configuration simulates composite reinforcements for a panel with multisite damage.

II. Finite Element Model

A typical composite patch-bonded repair consists of three elements: 1) the host aluminum panel, 2) the composite patch, and 3) the adhesive layer. The crack in the aluminum may lie inside or outside the patch. Because these three elements are very thin compared with their lateral dimensions, the use of three-dimensional finite elements is not practical. For efficiency, a double-plate model, developed by Sun et al.,[5] for calculating the stress-intensity factor in the cracked aluminum panel is employed.

The host aluminum panel and the composite patch are modeled as separate Mindlin plates connected by linear springs that represent the adhesive layer. Thus, at a planar nodal location, there are four nodes in the thickness direction, including two nodes for the adhesive spring. Displacement continuity along the aluminum–adhesive and adhesive–composite interfaces is achieved by linear constraint equations. The transverse shear deformation in the Mindlin plate theory provides a bilinear displacement approximation through the thickness of the host plate in the double-sided repair, when symmetry is involved in modeling.

The modified crack-closure technique[6] is used to calculate the strain energy release rate. It is assumed that the strain energy released during crack extension is equal to the work required to close the opened crack surfaces. It is also assumed that, when the aluminum crack reaches the composite repair, the adhesive will crack as well.

The strain energy release rate is computed for mode 1 fracture loading. The same procedure can be used for mixed-

Received Nov. 17, 1996; revision received Aug. 21, 1997; accepted for publication Oct. 6, 1997.

*Graduate Student, School of Aeronautics and Astronautics; currently at U.S. Air Force Wright–Patterson Air Force Base, OH 45433.

†Graduate Student, School of Aeronautics and Astronautics; currently Technical Staff, The Aerospace Corporation, El Segundo, CA 90245.

‡Neil A. Armstrong Professor of Aeronautical and Astronautical Engineering, 1282 Grissom Hall. Fellow AIAA.

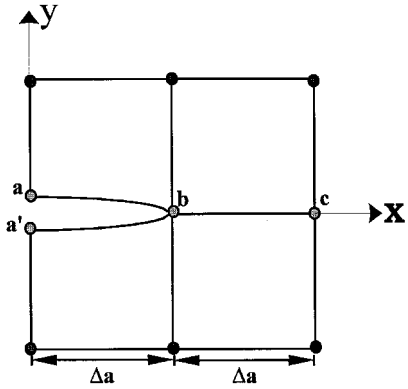

Fig. 1 Aluminum plate crack tip elements (top view).

mode loading. A four-noded Mindlin plate element is used to model the aluminum plate. The commercial finite element code ABAQUS is used to perform the finite element analysis with the four-noded thick-shell element. Figure 1 shows a two-dimensional finite element model for the aluminum plate near the crack tip at point b. Assume the crack front extends from b to c. Because the extension Δa is very small, the crack opening displacements at b are taken to be the same as those at a. Thus, the strain energy release rate can be calculated as the work done by the nodal force (moment) $F_y^b(M_x^b)$ in closing the crack-opening displacement (rotation) u_y^a (ψ_y^a). The total strain energy release rate is obtained as

$$\bar{G}_{\text{total}} = \bar{G}_u + \bar{G}_\psi = (1/2\Delta a)[F_y^b(u_y^a - u_y^{a'})] + (1/2\Delta a)[M_x^b(\psi_y^a - \psi_y^{a'})] \quad (1)$$

where $\bar{G}_u$, $\bar{G}_\psi$, and $\bar{G}_{\text{total}}$ are the translational, rotational, and total strain energy release rates, respectively. Note that these strain energy release rates are the respective energies released (over the total plate thickness) per crack tip.

The fracture parameter for the aluminum crack is often given in terms of the stress-intensity factor. The maximum (mode 1) stress-intensity factor is located on the tension side of the plate and is composed of

$$K = K_u + K_\psi\left(\frac{2z}{t_s}\right) = \sqrt{\frac{\bar{G}_u E_s}{t_s}} + \sqrt{\frac{3\bar{G}_\psi E_s}{t_s}}\left(\frac{2z}{t_s}\right) \quad (2)$$

where the subscript s denotes parameters associated with the aluminum plate; K_u is the stress-intensity factor as a result of the membrane action; and K_ψ is the stress-intensity factor as a result of bending. For symmetric repairs, it has been found that the variation of the stress-intensity factor through the plate thickness is small. Thus, the contribution of K_ψ to the stress-intensity factor is negligible.

With K determined as a function of crack length, numerical integration of the Paris law will give the fatigue life N as

$$N = \int_{a_i}^{a_f} \frac{da}{C(\Delta K)^m} \quad (3)$$

where a_i and a_f are the initial and final crack lengths, respectively; ΔK is the range of K during fatigue loading; and C and m are material properties. Typically, a Simpson's integration rule with at least 20 crack lengths is used for the integration.

Because there is a stress-intensity factor from both thermal residual stresses and mechanical load, the number of finite element runs can become quite high for parametric analysis of crack growth. Thus, a method of computing the stress-intensity factor by only two finite element runs at each crack length and respective geometry is presented. Only one finite element run is required to find a reference stress-intensity factor $(K_{\Delta T})_{\text{ref}}$ at a given reference value of temperature change $(\Delta T)_{\text{ref}}$, and a reference stress-intensity factor $(K_\sigma)_{\text{ref}}$ at a reference applied load $(\sigma_y)_{\text{ref}}$. For a given temperature change ΔT and an applied in-plane mechanical load σ_y, the stress-intensity factors in the aluminum plate are

$$K_{\text{thermal}}(a) = [\Delta T/(\Delta T)_{\text{ref}}][K_{\Delta T}(a)]_{\text{ref}} \quad (4)$$

$$K_{\text{mechanical}}(a) = [\sigma_y/(\sigma_y)_{\text{ref}}][K_\sigma(a)]_{\text{ref}} \quad (5)$$

respectively. Using superposition, the total stress-intensity factor as a function of crack length is the sum of the stress-intensity factors from the mechanical load and thermal residual stress, i.e.,

$$K(a) = K_{\text{mechanical}}(a) + K_{\text{thermal}}(a) \quad (6)$$

The R ratio of fatigue loading is defined as $R = K_{\min}/K_{\max}$. Thus, in a nominal tension–tension fatigue loading with vanishing minimum mechanical load, the R ratio may not vanish because of the presence of K_{thermal}. Therefore, the values of the coefficients C and m in the Paris law corresponding to the proper R ratio should be used. In the absence of such values, we follow the suggestion by Baker[7] to use $K_{\max}$ instead of ΔK in the Paris law, and retain the values of C and m for $R = 0$.

III. Specimen Preparation

Figure 2 shows the geometry of the reinforced double-edge-cracked specimen. This specimen was used to perform fatigue tests for generating crack growth data, which was used to determine the effective temperature drop ΔT_{eff} of the composite reinforcement. The aluminum alloy and the composite patch were 2024-T3 and AS4/3501-6 graphite/epoxy (Gr/Ep), respectively. The two slots were cut with a waterjet. The slots were not precracked prior to bonding, to prevent a possible reduction in stress-intensity through crack growth retardation. After bonding, a small notch was cut at the end of each slot with a jeweler's saw (0.008-in. blade) to sharpen the crack.

One of the most critical steps in the bonding procedure is the aluminum surface preparation. Reference 1 details the required steps of the aluminum preparation, which are briefly summarized as follows:

1) Surface degreasing: the aluminum surface of the repair area is thoroughly cleaned with methyl ethyl ketone.

2) Abrasion: the repair area is abraded with aluminum oxide abrasive paper to remove the oxide layer and expose a clean metal surface.

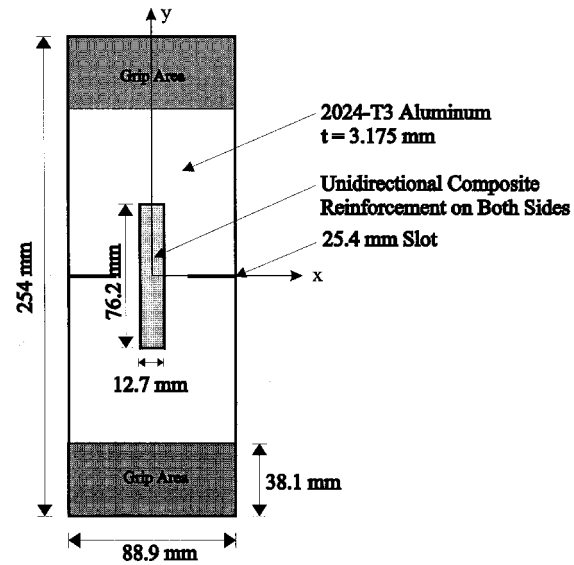

Fig. 2 Reinforced double-edge-crack specimen.

3) Primer: a 1% solution of silane primer (gamma–glycidoxypropyltrimethoxy silane) is brushed onto the repair area for 10 min. The specimen is then air-dried. The surface of the composite patch is only degreased and abraded.

Curing of the adhesive was done immediately following the aluminum surface treatment. FM73 (American Cyanamid) adhesive film was cured at 120°C for 1 h.[8]

IV. Results and Discussion

The first step in the analysis is to determine the effect of the thermal residual stresses. Conventionally, the value of ΔT is taken as the difference in the ambient room temperature of the component and the curing temperature. For a typical adhesive like FM73, the curing temperature is 120°C and ambient room temperature is 20°C, making a ΔT of -100°C. However, the actual value of ΔT is not well defined because of factors such as the adhesive not hardening at 120°C. Because of this uncertainty, an effective temperature drop ΔT_{eff} is proposed and defined as the temperature drop that can be adopted in a model without using temperature-dependent material properties.

Once the effective temperature drop is determined by comparing the finite element analysis to experimental results, a parameteric analysis can be performed to determine the effects of ply thickness and patch size on fatigue life. Finally, a simple model of the repair of multisite damage is proposed and analyzed with the effects of patch thickness on fatigue life.

A. Effect of Thermal Residual Stresses

The reinforced double-edge-cracked specimen is shown in Fig. 2. The composite reinforcement width is 12.7 mm. The reinforcement is Gr/Ep with the material properties given in Table 1. The thickness of each ply is 0.127 mm. The material properties for the aluminum and adhesive are shown in Table 2. The thicknesses for the aluminum and adhesive are 3.175 and 0.1 mm, respectively. Note that the thermal expansion of the adhesive is neglected.

First, a comparison of the experimental and finite element analysis fatigue life over the crack length of an unreinforced specimen is shown in Fig. 3. The experiment loading consists of a constant-amplitude tension–tension cyclic load at a peak load of 47.3 MPa (about one-tenth the yield stress of the aluminum) and an R ratio of 0. The material constants used in the Paris law [Eq. (3)] for aluminum 2024-T3 are $C = 4.086 \times 10^{-7}$ and $m = 2.318$, when K is in MPa $\sqrt{m}$ and the crack length is in mm/cycle.[9] The finite element analysis results using the given material constants together with the Paris law compare closely with the experimental results.

Before determining the value of ΔT_{eff}, the plate model shown in Fig. 4 is used to show the effect of thermal residual stresses on K for increasing crack length. Because of symmetry, only an eighth of the specimen is modeled. The thermal residual stresses lead to compression in the composite and tension in the aluminum, thereby leading to a residual stress-induced stress intensity.

Figure 5 shows the variation in K for different values of ΔT for two specimens reinforced with two and eight plies, respectively, of Gr/Ep on each side. The applied in-plane loading is 47.3 MPa. For the thicker eight-ply patch, the effect of thermal stresses is much more pronounced. Indeed, for a large temperature drop, the stress-intensity factor for the eight-ply repair may become much greater than for the two-ply repair, particularly at smaller crack lengths. In fact, at small crack lengths the stress-intensity factor is higher than that in the unpatched specimen if the temperature drop is large.

To determine ΔT_{eff}, the experimental results can be compared to a range of crack growth rate predictions that vary with ΔT. Tension–tension (with the mechanical $R = 0$) fatigue tests were conducted with specimens reinforced by two, four, six, and eight plies of Gr/Ep. Figures 6 and 7 show the experimental results for two- and eight-ply specimens, respectively. It is found that to properly fit these results using the finite element model, the magnitude of ΔT_{eff} is estimated to be -42°C. This value of effective thermal residual stress is below

Table 1 Composite material properties

Property	Gr/Ep	B/Ep
E_1, GPa	138	208
E_2, GPa	9.7	25.4
E_3, GPa	9.7	25.4
G_{12}, GPa	6.9	7.2
G_{13}, GPa	6.9	7.2
G_{23}, GPa	3.2	4.9
ν_{12}	0.3	0.1677
ν_{13}	0.3	0.1677
ν_{23}	0.49	0.035
α_1, 10^{-6} (°C)$^{-1}$	-0.7	4.5
α_2, 10^{-6} (°C)$^{-1}$	27.0	23.0
α_3, 10^{-6} (°C)$^{-1}$	27.0	23.0

Table 2 Aluminum and adhesive material properties

Property	Aluminum 2024-T3	Adhesive FM73
E, GPa	72.0	1.92
ν	0.3	0.27
α, 10^{-6} (°C)$^{-1}$	23.0	——

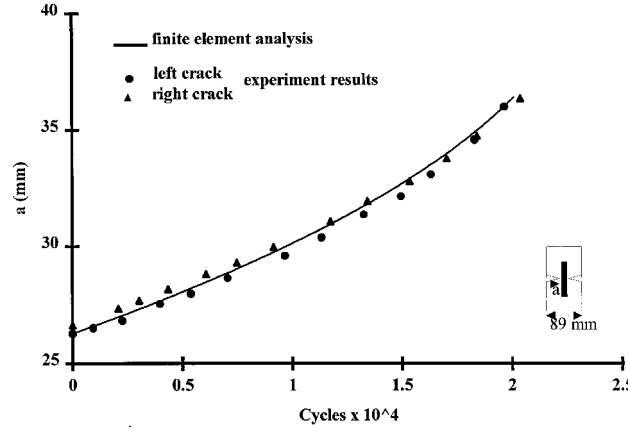

Fig. 3 Experimental results for unreinforced specimen.

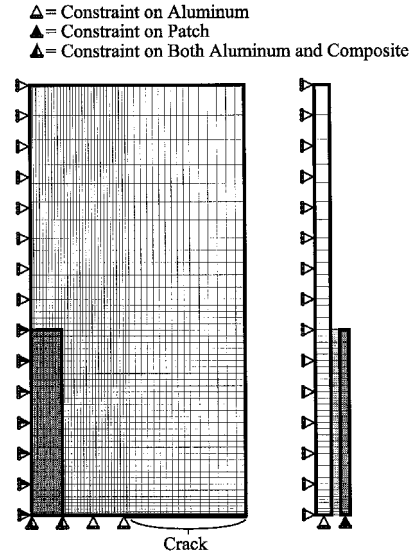

Fig. 4 Finite element model of reinforced specimen (a one-eighth model shown).

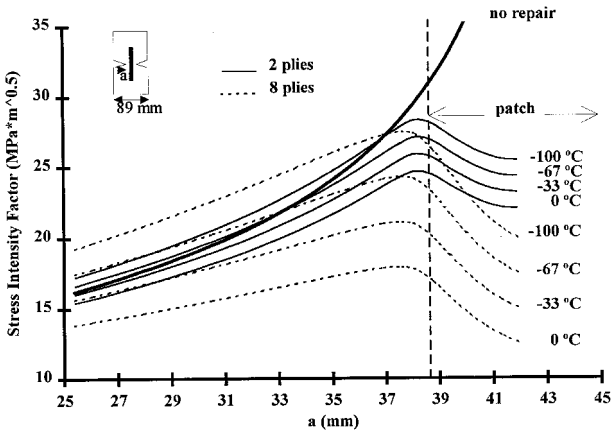

Fig. 5 Variation of K with number of composite plies and ΔT.

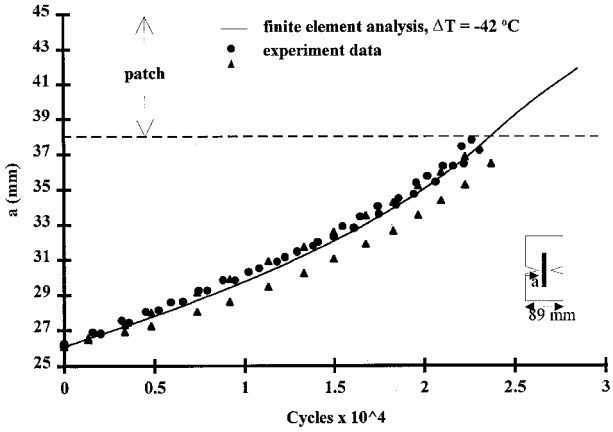

Fig. 6 Experimental results for two-ply Gr/Ep coupon specimens.

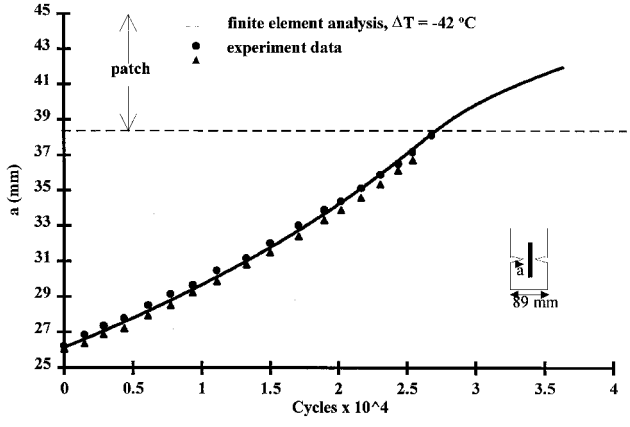

Fig. 7 Experimental results for eight-ply Gr/Ep coupon specimens.

the value using the cure temperature as the stress-free temperature. This is probably because of the use of temperature-independent material properties in the modeling and the hardening behavior of the adhesive while it cools.

With ΔT_{eff} determined, the actual effect of thermal stresses on the reinforced specimens is investigated. Figures 8 and 9 show how the stress-intensity is increased and fatigue life is consequently decreased by the presence of the thermal residual stresses. From Figs. 8 and 9, we observe that the reinforcement becomes most effective in reducing stress intensity after the crack begins to grow into the patched region. The crack growth rate does not decrease until the crack grows under the patch.

For the reinforced specimens tested and modeled here, the reinforcement does not have a great effect on fatigue life. However, this is a very harsh test of the reinforcement concept. The net cross-sectional area is drastically reduced as the cracks propagate toward each other. Also, the reinforcing composite patch is very narrow (only 12.7 mm).

B. Effect of a Wider Patch

To better demonstrate the effectiveness of the bonded composite reinforcement, a wider reinforcement is now considered. The width of the reinforcement is doubled, to 25.4 mm, using the same aluminum plate geometry. The applied load σ_y remains at 47.3 MPa. Figure 10 shows the finite element results for the reduction in stress intensity for both Gr/Ep and boron/epoxy (B/Ep) reinforcements. With a 10-ply Gr/Ep patch,

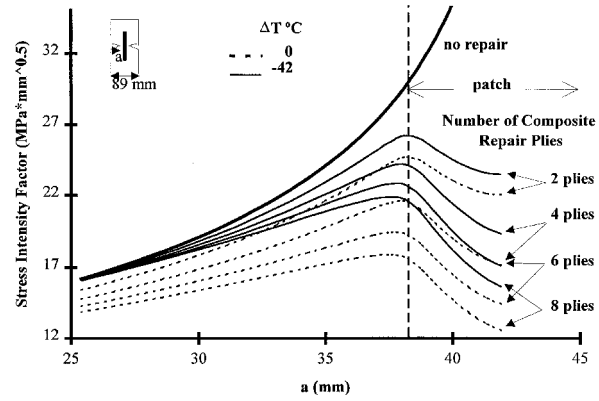

Fig. 8 Effect of ΔT_{eff} on K for Gr/Ep repairs.

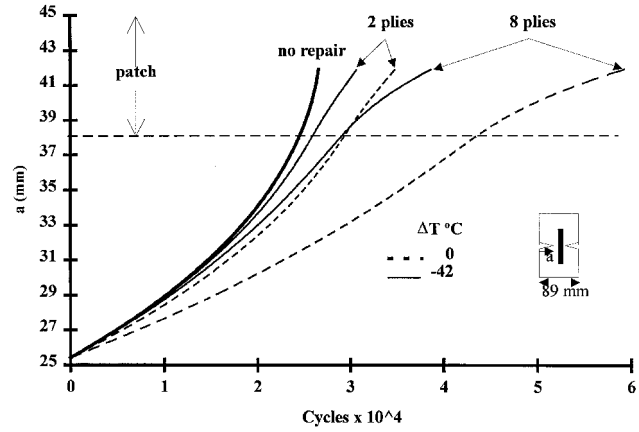

Fig. 9 Effect of ΔT_{eff} on fatigue crack growth for Gr/Ep repairs.

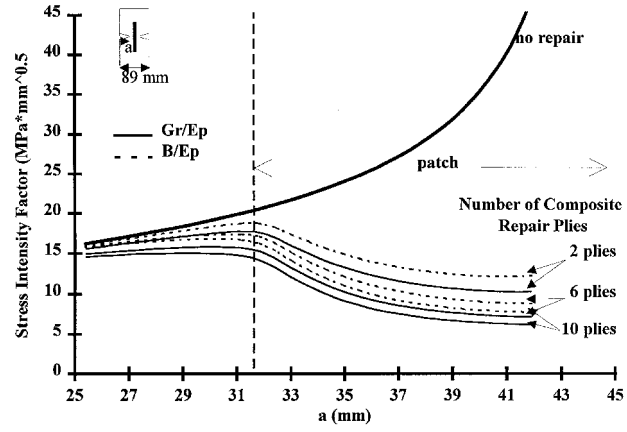

Fig. 10 Reduction in K with 25.4-mm-wide reinforcement patch.

there is an 83% reduction in K at a crack length of 42 mm. Ten plies of B/Ep are even more effective, with an 87% reduction. The plot also shows that the reinforcement is most effective after the crack begins to grow under the composite. After growing under the reinforcement, K is reduced lower than the initial value, even though the crack length is much longer.

Figure 11 shows the fatigue life results. The 10-ply Gr/Ep reinforcement results in a 500% increase in fatigue life, whereas the 10-ply B/Ep leads to a 785% increase at a crack length of 42 mm. Here, B/Ep is shown to be significantly more effective than Gr/Ep in increasing fatigue life. In fact, it is shown that the 6-ply B/Ep reinforcement is more effective in increasing the fatigue life than the 10-ply Gr/Ep. Ordinarily one would expect the reinforcement with the highest reinforcement-to-aluminum plate stiffness ratio S to have the longest fatigue life. However, the reinforcement-to-aluminum plate stiffness ratio is higher for the 10-ply Gr/Ep reinforcement than for the 6-ply B/Ep. This demonstrates the effect of the reduced thermal residual stress of the B/Ep over the Gr/Ep reinforcement. The thermal residual stress for the B/Ep reinforcement is lower as a result of both a reduced number of plies and a higher thermal coefficient in the fiber direction.

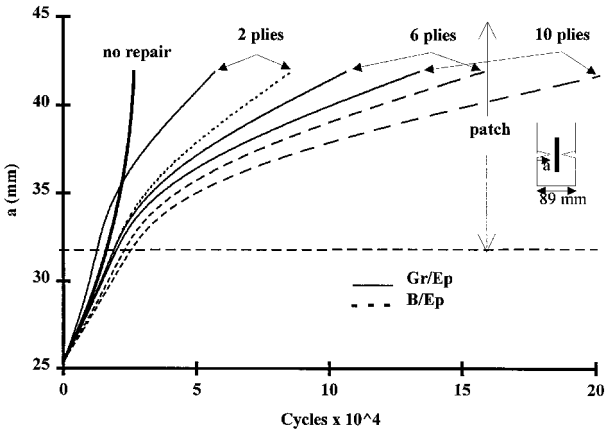

Fig. 11 Reduction in fatigue life with 25.4-mm-wide reinforcement patch.

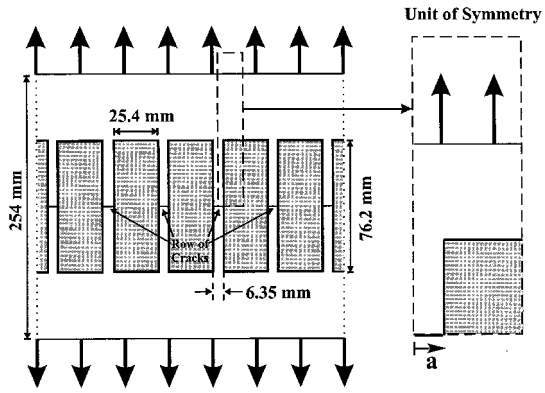

Fig. 12 Modeling of multiple-site damage.

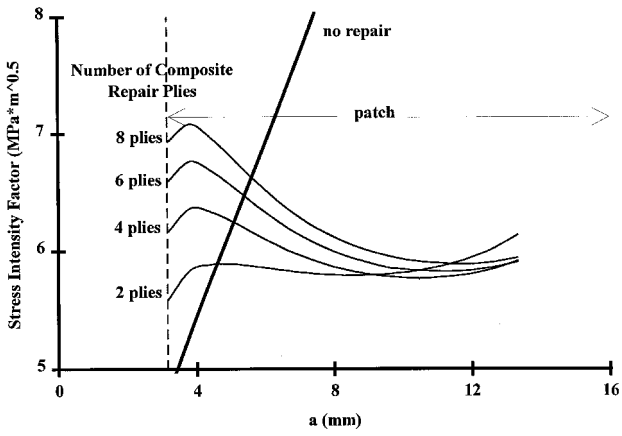

Fig. 13 Reduction in K for low applied load.

C. Multiple-Site Damage

The reinforced specimens considered in the previous sections, having only two colinear cracks, were designed with simple fabrication and testing in mind. To test a more pragmatic application of composite patch reinforcement, the finite element model was modified to consider a multiple-site damage problem. Figure 12 illustrates a row of identical cracked rivet holes, with the dashed-line box specifying a unit cell. With the appropriate boundary conditions applied, the infinite row is easily modeled in this way. Each of the cracked holes is modeled as a single crack that is 6.35 mm wide. The 25.4-mm strip between the adjacent cracks is completely covered by the bonded Gr/Ep composite patch. All of the cracks are assumed to grow simultaneously.

Figure 13 shows the reduction in K for a relatively low tensile load of $\sigma = 47.3$ MPa. It is noted that thicker reinforcements are not necessarily more effective in reducing the stress-intensity factor. The greater thermal residual stresses induced by the thicker composite may override the benefits resulting from its greater stiffness.

However, for higher loads, thicker reinforcements definitely provide greater crack arrestment capability. This is clearly demonstrated by the results shown in Figs. 13 and 14 for a load of $\sigma_y = 141$ MPa, which is about one-third the yield stress.

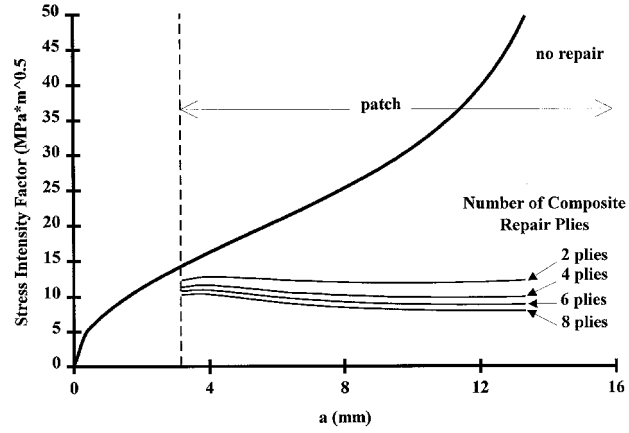

Fig. 14 Reduction in K for high applied load.

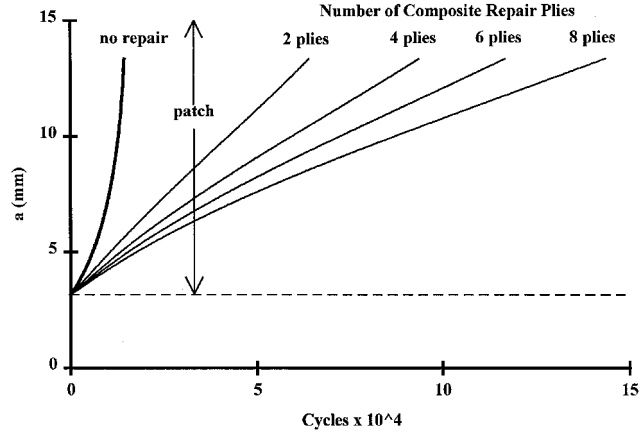

Fig. 15 Increase in fatigue life for high load.

For this load level, the effect of thermal residual stress becomes less pronounced. In Fig. 15, note that, for a crack length of 13 mm, an 84% reduction in K and a 1000% increase in fatigue life are gained with the eight-ply Gr/Ep reinforcement.

The most important benefit of this type of reinforcement is that, even with crack growth, stress intensity can be held well below the fracture toughness. If the integrity of the adhesive bond is maintained, then no catastrophic failure by consecutive linking of the small colinear cracks will be achieved.

V. Conclusions

In this study, the concept of using bonded composite patches as reinforcements for preventing crack coalescence in cracked aluminum panels is investigated. The reinforcements are shown to be able to increase fatigue life and protect against catastrophic failure. Thermal residual stresses in the aluminum panel, induced during bonding, can significantly affect the effectiveness of patching and, therefore, must be accurately determined. For aluminum alloy 2024-T3, AS4/3501-6 Gr/Ep reinforcement, and FM73 adhesive, the effective stress-free temperature is estimated to be $-42°C$. For lower mechanical loads, the thermal residual stresses may dominate and produce adverse effects on fatigue crack growth. At higher loading levels, the effect of thermal residual stresses can become insignificant. It is also demonstrated that the reinforcement could be applied to the multiple-site damage problem with excellent results.

Acknowledgments

This work was supported by the U.S. Air Force Office of Scientific Research through University Research Initiative Grant F49620-93-0377 to Purdue University. Walter Jones was the Grant Monitor.

References

[1]Baker, A. A., and Jones, R., *Bonded Repair of Aircraft Structures*, Martinus–Nijhoff, Dordrecht, The Netherlands, 1988.

[2]Jones, R., and Smith, W. R., "Continued Airworthiness of Composite Repairs to Primary Structures for Military Aircraft," *Composite Structures*, Vol. 33, No. 1, 1995, pp. 17–26.

[3]Belason, E., "Bonded Doublers for Aircraft Structure Repair," *Aerospace Engineering*, July 1995, pp. 13–18.

[4]Park, J. H., Ogiso, T., and Atluri, S. N., "Analysis of Cracks in Aging Aircraft Structures, With and Without Composite-Patch Repairs," *Computational Mechanics*, Vol. 10, Nos. 3, 4, 1992, pp. 169–201.

[5]Sun, C. T., Klug, J. C., and Arendt, C., "Analysis of Cracked Aluminum Plates Repaired with Bonded Composite Patches," *AIAA Journal*, Vol. 34, No. 2, 1996, pp. 369–374.

[6]Rybicki, E. F., and Kanninen, E. F., "A Finite Element Calculation of Stress Intensity Factors by a Modified Crack Closure Integral," *Engineering Fracture Mechanics*, Vol. 9, No. 9, 1977, pp. 931–938.

[7]Baker, A., "Growth Characterisation of Fatigue Cracks Repaired with Adhesively Bonded Boron/Epoxy Patches," *Proceedings of the 9th International Conference on Fracture, Advances in Fracture Research*, edited by B. L. Karihaloo, Y.-W. Mai, M. I. Ripley, and R. O. Ritchie, Pergamon, New York, Vol. 1, 1977, pp. 117–128.

[8]Chiu, W. K., Chalkley, P. D., and Jones, R., "Characterization of FM73 Film Adhesive," *Proceedings of the International Conference on Aircraft Damage Assessment and Repair*, 1991, pp. 409–414.

[9]E. P. Phillips, "Long Crack Growth Rate Data—Constant Amplitude and FALSTAFF Loading," *Short-Crack Growth Behavior in an Aluminum Alloy*, edited by J. C. Newman Jr. and P. R. Edwards, AGARD Cooperative Test Programme, Rept. 732, AGARD, 1988, pp. 78–83.